Evidence for Flexibility in the Function of Ribonuclease A[†]

Roger Cole and J. Patrick Loria*

Department of Chemistry, Yale University, P.O. Box 208107, New Haven, Connecticut 06520

Received February 8, 2002; Revised Manuscript Received March 20, 2002

ABSTRACT: The dynamic properties of the enzyme ribonuclease A (RNase A) were investigated through the use of solution NMR spin relaxation experiments. As determined by "model-free" analysis, RNase A is conformationally rigid on time scales faster than overall rotational tumbling (picoseconds to nanoseconds). The average order parameter, S^2, for RNase A is 0.910 ± 0.051. However, 28 of the amino acid residues in RNase A were identified as undergoing chemical exchange on the microsecond to millisecond time scale. For 16 of these residues the microscopic chemical exchange rates, k_{ex}, were quantitated through the use of the relaxation-compensated CPMG (rcCPMG) experiment. The value of k_{ex} was identical for all residues with an average of 1640 s^{-1} and is similar to the RNase A k_{cat} value of 1900 s^{-1}. Many of these mobile residues localize to the active site in RNase A and include the catalytically crucial amino acids His119 and Asp121. Additional motion is found in the B1, B2, and P0 subsites, suggesting a coupling of motion between the binding and catalytic sites. The activation energy of the observed millisecond motion was measured by applying the rcCPMG experiment at temperatures of 283, 293, and 298 K and was determined to vary between 3.6 and 7.4 kcal/mol. The measured barrier to conformational motion is similar to the activation barrier for the RNase A catalyzed reaction and thus would not be thermodynamically limiting to catalysis. These studies suggest a correlation of conformational exchange kinetics and thermodynamics derived from NMR measurements with those determined by biochemical means and are suggestive of an important role for flexibility in enzyme function.

Proteins undergo a variety of dynamical fluctuations that occur over a wide range of time scales (*1*). Perhaps the most vivid experimental evidence demonstrating the existence of motion has been the "before and after" time-averaged structures of proteins in the apo- and ligand-bound states as determined by solution nuclear magnetic resonance (NMR) spectroscopy and X-ray crystallography (*2*−*6*). These time-dependent excursions between different conformational substates are essential for protein function, and therefore their characterization is of paramount importance. Many biological processes occur on time scales ranging from 10^7 to 10^1 s^{-1} (*1*, *7*, *8*), and solution NMR spin relaxation experiments are uniquely suited for characterizing motions of these frequencies (*9*−*11*).

By design, enzymes possess enough structural flexibility to accommodate binding of substrates, reaction intermediates, and products and thus represent attractive molecules in which to characterize the role of protein fluctuations in biological function. Here we describe our initial efforts at investigating the conformational plasticity of bovine pancreatic ribonuclease A (RNase A).[1] RNase A (EC 3.1.27.5) is a remarkably well-studied enzyme (for reviews see refs *12* and *13*). There are over 100 three-dimensional structures of RNase A, determined by both homonuclear solution NMR and X-ray crystallography, in the protein data bank (PDB) (*14*). Recently, interest in RNase A has increased due to the reported cytotoxic properties of RNase A (*15*). Despite the abundance of biochemical data and the clinical importance of this enzyme, its dynamical properties have yet to be characterized in detail.

RNase A is a 124-residue, highly stable (*16*), monomeric protein enzyme that catalyzes the cleavage of the P−$O^{5'}$ bond in single-stranded RNA. The enzyme does not require metal ions or cofactors for activity. Catalysis entails cleavage on the 3′-phosphate side of pyrimidines, yielding an RNA−pyrimidine 3′-phosphate and ribonucleic acid containing a 5′-OH group. The enzyme active site resides in a deep cleft, and interactions between RNase A and substrates (or inhibitors) occur through distinct binding subsites (Scheme 1) (*17*, *18*).

The B1 subsite (base binding site) is specific for binding the pyrimidine base that is 5′ to the scissile phosphate group and has a kinetic preference for cytosine relative to uracil (*19*, *20*). Specificity at this site is determined primarily by Thr45 and Asp83. The B2 subsite provides a binding pocket for the leaving group nucleotide portion of the substrate and

[†] Funding from the Camille and Henry Dreyfus Foundation and American Cancer Society (IRG 58-012-42) is gratefully acknowledged by J.P.L. R.C. thanks the National Science Foundation for a Graduate Research Fellowship.

* Corresponding author: 203-436-4847 (phone); 203-432-6144 (fax); patrick.loria@yale.edu (e-mail).

[1] Abbreviations: RNase A, bovine pancreatic ribonuclease A; CPMG, Carr−Purcell−Meiboom−Gill R2 experiment; rcCPMG, relaxation-compensated CPMG; τ_{cp}, time between 180° ^{15}N CPMG refocusing pulses; $R_2(1/\tau_{cp})$, transverse relaxation rate measured as a function of CPMG refocusing delay; CSA, chemical shielding anisotropy; $\Delta\omega$, chemical shift difference between nuclei involved in two-site conformational exchange; $p_{a/b}$, population of equilibrium sites for a two-site ($A \leftrightarrow B$) exchange mechanism; R_{ex}, excess line broadening of a NMR resonance due to chemical exchange; k_{ex}, rate constant for conformational exchange between two sites.

10.1021/bi025655m CCC: $22.00
Published on Web 04/17/2002

Scheme 1: Diagram of the Ribonuclease A Active Site[a]

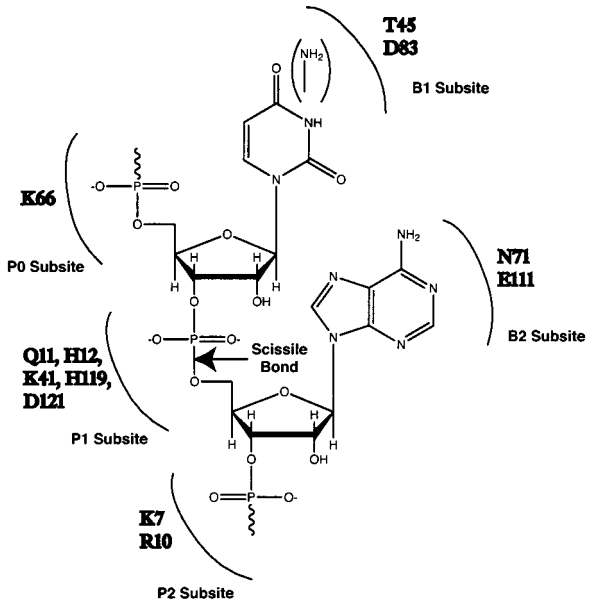

[a] The RNase A active site pocket is shown in 2D representation. The base and phosphate binding subsites are indicated with B*x* and P*x*, respectively. Conserved residues important for substrate binding and/or catalysis are indicated with the one-letter amino acid code nearest the subsite in which they reside. The phosphate bond cleaved during the RNase A catalyzed reaction is indicated with an arrow. As depicted, RNase A has an absolute requirement for pyrimidines (uracil and cytosine are shown) at the B1 site and a strong preference for adenine at the B2 subsite (*94*). This scheme is closely adapted from ref *13*.

has a preference for binding adenine (*21*). Residues located at or near the B2 subsite include Asn71, Glu111, Thr70, and Gln69. The B3 subsite demonstrates a preference for purine bases, and its existence has been determined by kinetic experiments (*22*). The P0 subsite (phosphate binding site) and P2 subsite both contain highly conserved residues such as Lys66 and Arg10, respectively. These cationic residues interact favorably with the anionic phosphates of enzyme-bound RNA. Located at the P1 subsite are the residues that are directly involved in facilitating phosphate cleavage.

Early in the study of RNase A it was demonstrated that enzyme catalysis relies heavily on the action of two species invariant residues: His12 and His119. Histidine 12 acts as a base to abstract a proton from the 2′-OH of the ribose facilitating its in-line attack on the phosphorus atom. The side chain of His119 donates a proton to the 5″-oxygen of the leaving group forming a 2′,3′-cyclic intermediate. Both cleavage products are then released to solvent. The hydrolysis of the 2′,3′-cyclic intermediate occurs in a reaction that is the reverse of the transphosphorylation step. Catalysis by RNase A is aided by the action of other important residues. The N_ζ atom of Lys41 and the backbone amide N−H group of Phe120 stabilize the pentacoordinate transition state ($TS^{\ddagger}$) in the RNase A reaction by interacting with the trigonal-bipyramidal nonbridging phosphate oxygens (*23*).

Because of the detail in which RNase A has been studied, evidence exists of dynamic processes in the functioning of this enzyme. Several X-ray crystallographic and NMR spectroscopic studies have suggested the presence of conformational motion at the active site of RNase A. For instance, His119 has been shown to exist in two distinct equilibrium conformations designated A and B, the result of a 180° rotation about the $C_\alpha-C_\beta$ bond (*24*−*30*). Histidine 119 must be in position A for the transphosphorylation reaction to occur; however, hydrolysis can occur with His119 in either position A or B. Conformation A is apparently stabilized by hydrogen-bonding interactions between the imidazole nitrogen of His119 and the side chain carboxyl of the highly conserved Asp121 (*31*, *32*). Thus, the conformational fluctuations of His119 appear to bear directly on RNase A catalytic activity. Interestingly, NOE restraints from solution NMR studies are incompatible with a single protein conformer and instead suggest the presence of two structures in equilibrium (*28*, *33*). Additional evidence for the existence of a two-state dynamic equilibrium of RNase A was provided by Hammes and co-workers using temperature-jump experiments (*34*). In these studies a conformational change occurs in RNase A with a rate constant of 3500 s^{-1} and is ascribed to a carboxyl−histidine interaction (*34*). Despite the evidence for flexibility in RNase A (*32*, *35*−*39*), its motional behavior has yet to be thoroughly characterized in atomic detail.

We demonstrate here, through the implementation of NMR spin relaxation experiments, that microsecond to millisecond motion is occurring throughout RNase A, including active site residues. This motion occurs on a time scale of biological relevance. We further demonstrate that RNase A is quite immobile in the picosecond to nanosecond time window.

EXPERIMENTAL PROCEDURES

Protein Expression and Purification. Escherichia coli strain BL21(DE3) was from Novagen (Madison, WI). All buffers and salts were from Sigma Chemical Co. (St. Louis, MO). The plasmid pBXR encoding for bovine pancreatic ribonuclease A was a generous gift of Professor Ronald T. Raines (University of Wisconsin−Madison). Isotopically labeled RNase A was expressed and purified according to published protocols (*40*) with the modification that the final growth was performed in M9 media containing 1 g/L $[^{15}N]NH_4Cl$ and either [^{12}C]- or [^{13}C]glucose and supplemented with vitamins and trace metals. Ribonuclease was purified and refolded by the method outlined by Raines and co-workers (*40*). The purified RNase A was determined to be >98% pure. For NMR experiments, RNase A was dialyzed exhaustively against deionized water and concentrated in an Amicon centricon, the pH was adjusted to 6.4, and the ionic strength was held constant at 10 mM NaCl.

Solution NMR Experiments. Backbone and side chain resonance assignments of RNase A have been performed previously at acidic pH (*39*). We have reassigned the resonances in the enzyme at pH = 6.4 and pH = 4.5 using three-dimensional HNCA (*41*), HN(CO)CA (*42*), HNCACB (*43*), CBCA(CO)NH (*44*), ^{1}H−^{15}N TOCSY-HSQC, and ^{1}H−^{15}N NOESY-HSQC experiments (*45*−*47*) and interproton distances derived from the crystal structure [PDB 7RSA (*48*)] using in-house written software.

All NMR spin relaxation experiments were performed on a 600 μM ^{15}N RNase A (pH = 6.4) sample on a four-channel Varian Inova 600 MHz instrument equipped with a triple-resonance probe with three-axis pulsed field gradients. Sensitivity-enhanced gradient-selected experiments were used for longitudinal (R_1) and transverse (R_2) relaxation experi-

ments and heteronuclear NOE experiments (*49*−*51*). The heteronuclear NOE experiments were performed by interleaving experiments with and without proton saturation to minimize the effects of environmental fluctuations. The R_1 experiments were performed with relaxation delays of 2 (×2), 82, 172, 282 (×2), 412, 812 (×2), and 1222 ms. The R_2 experiments were performed with relaxation delays of 0 (×2), 12, 28, 44 (×2), 62, 86, 112 (×2), 148, 198, and 250 ms. Two-dimensional spectra were acquired with 2162 × 128 complex points in the t_2 and t_1 dimensions with corresponding spectral widths of 12000 and 1800 Hz. The proton RF carrier was set coincident with the water resonance, and the ^{15}N carrier frequency was at 119 ppm. Prior to Fourier transformation, resolution enhancement was performed using Lorentz-to-Gauss processing in t_2 followed by zero filling. In t_1, the data were extended by a factor of 2 by linear prediction, a Kaiser window function was applied, and the subsequent data were zero filled and Fourier transformed. Each experiment was processed with NMRpipe (*52*) and visualized with Sparky (*53*). Peak intensities, from a 3 × 3 grid, were extracted from the Sparky 2-D matrices and fitted to a single exponential decaying function by a nonlinear least-squares routine using in-house written software and Curvefit (kindly proved by Professor Arthur G. Palmer, Columbia University).

To determine the chemical exchange contribution to the NMR resonance line width, R_{ex}, and the microscopic rate constant, k_{ex}, the relaxation-compensated CPMG experiment (rcCPMG) was performed as a function of interpulse delay, τ_{cp} (*54*). Values of $R_2(1/\tau_{cp})$ were determined at τ_{cp} delays of 1, 1.32, 2, 2.8, 4.6, and 10 ms as described (*54*). The exchange rate constant, k_{ex}, for nuclei in equilibrium between two magnetically inequivalent sites (A ↔ B) is equal to the sum of the forward and reverse rate constants, k_1 and k_{-1}. The value of $R_2(1/\tau_{cp})$ for all time scales is given by (*55*, *56*)

$$R_2(1/\tau_{cp}) = \frac{1}{2}\left(R_{2A}^0 + R_{2B}^0 + k_{ex} - \frac{1}{\tau_{cp}}\cosh^{-1}[D_+\cosh(\eta_+) - D_-\cos(\eta_-)]\right) \quad (1)$$

$$D_\pm = \frac{1}{2}\left[\pm 1 + \frac{\Psi + 2\Delta\omega^2}{(\Psi^2 + \zeta^2)^{1/2}}\right] \quad (2)$$

$$\eta_\pm = \frac{\tau_{cp}}{\sqrt{2}}[\pm\Psi + (\Psi^2 + \zeta^2)^{1/2}]^{1/2} \quad (3)$$

$$\Psi = (R_{2A}^0 - R_{2B}^0 - p_A k_{ex} + p_B k_{ex})^2 - \Delta\omega^2 + 4p_A p_B {k_{ex}}^2 \quad (4)$$

$$\zeta = 2\Delta\omega(R_{2A}^0 - R_{2B}^0 - p_A k_{ex} + p_B k_{ex})$$

in which $R_{2A/B}$ and $p_{A/B}$ refer to the transverse relaxation rate and the equilibrium populations for site A or B and $\Delta\omega$ is the chemical shift difference between the exchanging sites. A simplified expression valid for $p_A \gg p_B$ is given by (*57*)

$$R_2(1/\tau_{cp}) = R_2(1/\tau_{cp}\rightarrow\infty) + p_A p_B \Delta\omega^2 k_{ex}/[{k_{ex}}^2 + ({p_A}^2\Delta\omega^4 + 144/{\tau_{cp}}^4)^{1/2}] \quad (5)$$

Table 1: Summary of Conformational Exchange Kinetics[a]

residue	R_{ex} (s^{-1})	k_{ex} (s^{-1})	secondary structure
Met13	3.2 ± 0.5	1530 ± 680	coil
Ser15	7.5 ± 1.4	1020 ± 580	coil
Ser22	22.1 ± 0.9	1620 ± 160	coil
Phe46	24.1 ± 0.5	1540 ± 130	β1
Ser50	1.3 ± 0.4	1200 ± 630	coil
Ala64	1.7 ± 0.6	1100 ± 710	coil
Cys65	4.1 ± 0.3	1180 ± 320	coil
Lys66	33.8 ± 9.7	3380 ± 1520	coil
Gln69	10.2 ± 0.7	1700 ± 240	coil
Asn71	20.0 ± 1.5	1990 ± 410	β3
Thr78	2.6 ± 0.8	1540 ± 650	coil
Ser80	3.4 ± 0.9	1230 ± 580	β4
Thr100	8.6 ± 1.0	1580 ± 220	β5
Ala109	9.0 ± 2.8	3090 ± 1430	β5
His119	13.9 ± 2.0	1110 ± 230	β6
Asp121	6.0 ± 2.8	1460 ± 1190	β6

[a] Secondary structure elements are defined by the program MolMol (*93*). The terms bridge, turn, coil, and bend output by MolMol are listed above under the inclusive term coil.

In the limit of fast chemical exchange ($k_{ex} > \Delta\omega$), the dependence of $R_2(1/\tau_{cp})$ on $1/\tau_{cp}$ is shown by eq 6 (*58*, *59*).

$$R_2(1/\tau_{cp}) = R_2(1/\tau_{cp}\rightarrow\infty) + (p_A p_B \Delta\omega^2/k_{ex})[1 - 2\tanh(k_{ex}\tau_{cp}/2)/(k_{ex}\tau_{cp})] \quad (6)$$

Analysis of conformational exchange through fitting of $R_2(1/\tau_{cp})$ is referred to as dispersion analysis. With rcCPMG data at a single static magnetic field, the relaxation dispersion data were fit to eq 6 as described previously (*54*, *58*). In the absence of data from multiple magnetic fields, we justify our use of eq 6 on the following basis. (1) We used the average value of $k_{ex} = 1600\ s^{-1}$ (vide infra) and values of $p_A = 0.95$ and $p_B = 0.05$ in conjunction with eq 5 to estimate an approximate value of $\Delta\omega$. For all residues in Table 1, values of $\Delta\omega$ were less than the k_{ex} values determined using eq 6; these simulated values of $\Delta\omega$ ranged from 200 to 1000 s^{-1} (0.5−2.9 ppm). The ratio of k_{ex}:$\Delta\omega$ ranged from 2 to 6, indicating that $k_{ex} > \Delta\omega$ under these conditions. (2) Values for $\Delta\omega$ of ^{15}N nuclei have been reported for other proteins and range from <1 to 4 ppm (*59*, *60*) and are similar to the $\Delta\omega$ values estimated herein. These values for $\Delta\omega$ are less than the values of k_{ex} determined from fitting to eq 6 and subsequently reported in Table 1, further supporting the use of the fast limit equation. (3) Finally, fitting the relaxation data to eq 1 gives values of $\Delta\omega$ that are less than calculated k_{ex} values for 14 of 16 residues, indicating fast exchange conditions. Exchange rate constants for these 14 residues are essentially identical to those calculated using eq 6. For 12 of the 16 exchanging residues fitting of the data to eq 1 results in no decrease in χ^2 values, indicating use of the general exchange model is not warranted in this case. For two of the residues, His119 and Lys66, a slight improvement in χ^2 values is observed from 1.7 to 0.8 and from 3.5 to 2.2, respectively, upon fitting to eq 1. *F*-statistical testing indicates that these decreases in χ^2 are not significant. For the two residues (Asp121 and Ser80) where *F*-tests indicate that the use of eq 1 in fitting the data is more appropriate, fitting to eq 1 gives unreasonable values for k_{ex} and populations. For example, the results for fitting relaxation data for Asp121 to eq 1 give populations of 55% and 45% for conformation

A and B with k_{ex} values of 10 s^{-1} and $\Delta\omega$ of 230 Hz. Similar results are observed for Ser80. These values would suggest two peaks in slow exchange of roughly similar intensity. We never observe two peaks for Ser80 or Asp121 in our 2D or 3D experiments. Also, this value of k_{ex} is over 2 orders of magnitude less than all other residues in RNase A. The results of fitting relaxation data for all residues, except Ser80 and Asp121, to eq 1 give an average population for site A of 97%, not 55%. Taken together, these results suggest that the statistical improvement in fitting the data to eq 1 is not real, and therefore all parameters reported herein result from fitting the data to the fast limit equation (eq 6).

Model-Free Analysis. Fast time scale motions were analyzed by fitting NMR spin relaxation rates to one of five semiempirical forms of the spectral density function using the "model-free" analysis (*61*, *62*). Each form of the spectral density function is comprised of terms that directly describe the motion of a bond vector on the picosecond to nanosecond time scale. Fitting of motional parameters to the spin relaxation data was performed using the program "Model-Free 4.01" (*63*, *64*). Model selection was based on the statistical testing protocol described previously by Mandel et al. (*63*). Prior to model-free analysis, the rotational diffusion tensor for RNase A was estimated by R_2/R_1 ratios and the program "R2R1_diffusion" and from the X-ray crystal structure [7RSA (*48*)] in which hydrogens had been added using the program Insight97 (MSI) with the program "pdbinertia" (provided by Professor Arthur G. Palmer, Columbia University). During the model-free analysis, N−H bond lengths were assumed to be 1.04 Å, and the ^{15}N chemical shift anisotropy was estimated as −162 ppm. For each model, 500 randomly distributed data sets were generated. Models were selected by comparing the sum-squared error of the optimal fit with the 0.05 critical value of the distribution. In cases where *F*-statistics were applicable, comparisons were made with the 0.20 critical value of the distribution. During the model selection process, the diffusion tensor parameters were kept fixed. Once models had been assigned to each spin, both the diffusion tensor and model parameters were optimized simultaneously. The process of model selection was then repeated until the optimized tensor parameters did not differ significantly from those used during the previous round of model selection.

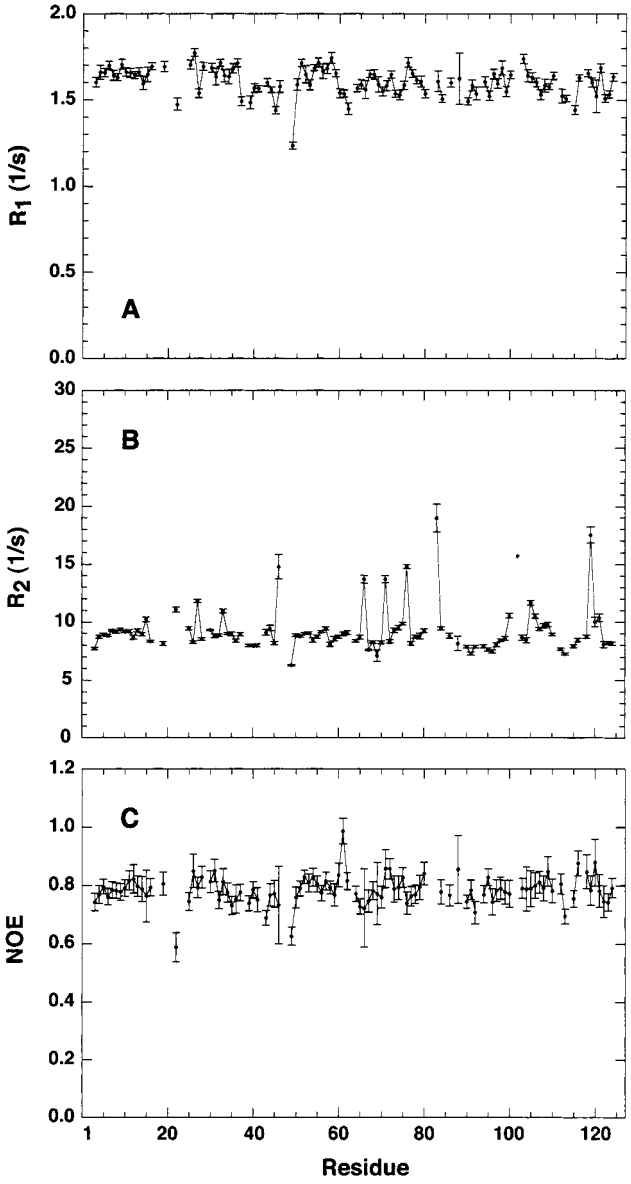

FIGURE 1: [^{15}N]Amide spin relaxation rates at 14.1 T. (A) R_1, (B) R_2, and (C) heteronuclear NOE values are plotted versus the ribonuclease A amino acid sequence. All NMR experiments were performed at 298 K as described in Experimental Procedures. Gaps in the connecting lines indicate residues where no data are available due to overlap or low signal to noise in the peak intensity.

RESULTS

Fast Time Scale Motions (Picoseconds to Nanoseconds). We chose a pH of 6.4 for the present study because this value is at the low pH edge of the plateau region of the enzyme activity vs pH profile, thereby allowing study of RNase A in its most enzymatically active state (*65*). It is noteworthy that several residues in RNase A undergo significant amide chemical shift changes relative to those determined at low pH values (see Supporting Information). Several of these residues, including Gln11, Asp83, and His119, are located at the active site.

The spin relaxation behavior of 97 of the 120 non-proline residues in RNase A could be reliably quantitated. T17, S18, M29, V47, H48, V63, T82, D83, R85, G88, Q101, and E111 were of low intensity or overlapped with other residues, and K1, E2, S16, A20, S21, S23, N24, D38, I81, S89, and A102 were not present in 2D $^1H-^{15}N$ HSQC spectra. These residues were excluded from further analysis. The average values of the relaxation rates (10% trimmed) are $R_1 = 1.61 \pm 0.01$ s^{-1}, $R_2 = 8.74 \pm 0.47$ s^{-1}, and NOE = 0.784 ± 0.019. Plots of these relaxation rates are shown in Figure 1. It is interesting to note that the values of the heteronuclear NOE for residues at the N- (residues 3−5; NOE = 0.769 ± 0.026) and C-terminus (residues 121−124; NOE = 0.766 ± 0.025) are similar to those in the remainder of the protein. This is likely the result of close packing of these regions with the rest of the protein and the importance of the N-terminal sheet (β6) and C-terminal helix (α1) in substrate binding and the catalytic reaction. Also of note are the elevated values of the transverse relaxation rate constants (Figure 1B) in distinct protein regions, suggesting areas of conformational exchange.

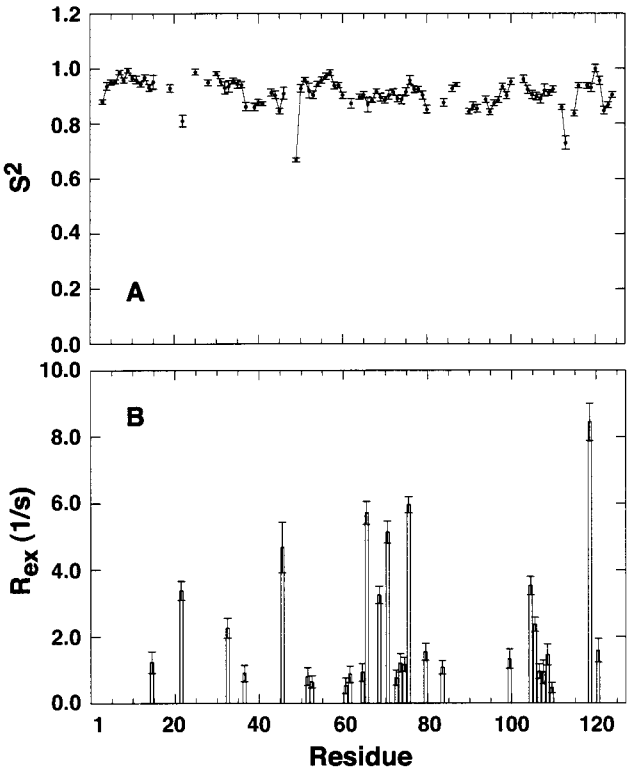

FIGURE 2: RNase A dynamics from model-free analysis. (A) Generalized order parameter, S^2, and (B) residues undergoing conformational exchange. In (A), S^2 values determined at 298 K are plotted as a function of amino acid sequence. In (B), residues for which model 3 or 4, containing an R_{ex} term, was an appropriate description of the spin relaxation data are plotted.

Rapid amide N−H bond vector motions that modulate the dipolar and chemical shift anisotropy (CSA) interactions were analyzed by the model-free protocol using NMR spin relaxation data (*61*, *62*). Of the 97 residues whose relaxation rates could be reliably quantitated, 95 were fit to models 1−5. The spin relaxation behavior of Cys26 and Asn27 could not be adequately described by any of the models. Model 1 (S^2) was an appropriate fit for 58 residues, 8 residues fit to model 2 (S^2 and τ_e), 27 residues fit to model 3 (S^2 and R_{ex}), 1 fit to model 4 (S^2, τ_e, and R_{ex}), and 1 residue fit to model 5 (S^2_f, S^2_s, and τ_e). Tables summarizing the results of the model-free fitting are provided in the Supporting Information. The spin relaxation data were best fit in the context of an axially symmetric rotational diffusion tensor for RNase A with $D_{\parallel}/D_{\perp} = 0.84 \pm 0.01$, $\Phi = 150.3 \pm 12.3°$, and $\Theta = 14.9 \pm 3.0°$ and a rotational correlation time of 6.49 ± 0.01 ns. Excluding residues with elevated R_2 values (10% trimmed mean), an estimate of the rotational correlation time at 298 K for RNase A is 6.74 ± 0.04 ns as determined from the ratio of the ^{15}N transverse and longitudinal relaxation rates and 6.3 ns as determined from the Stokes−Einstein equation using a 13.7 kDa spherical protein with a 3.2 Å water hydration shell. These data indicate that RNase A is monomeric in solution. The generalized order parameters (S^2) determined from model-free fitting are plotted as a function of amino acid sequence in Figure 2 (*61*, *62*). The calculated order parameters are high and relatively uniform across the RNase A sequence, suggesting a stable rigid protein on this time scale. The average order parameter for the entire protein is $0.910 \pm 0.051$with secondary structure elements showing the expected behavior: α-helix $= 0.954 \pm 0.023$, β-sheet $= 0.908 \pm 0.035$, and loops and turns $= 0.888 \pm 0.058$. Ser22, Glu49, and Asn113 have order parameters that deviate significantly from the rest of the protein. In Figure 3, the values of S^2 are mapped onto the three-dimensional ribbon structure of RNase A.

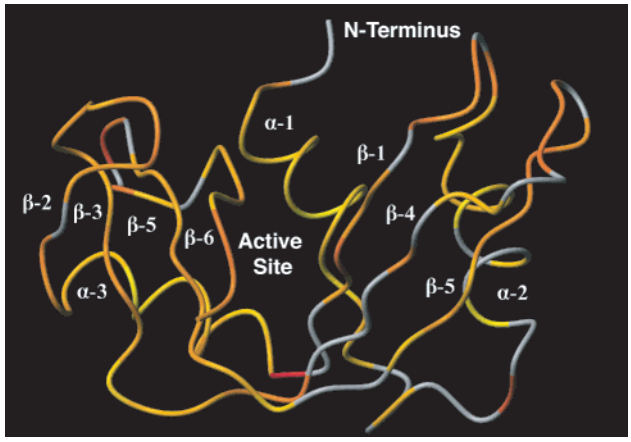

FIGURE 3: Depiction of RNase A order parameters. S^2 values are color coded onto the RNase A structure [PDB 7RSA (*48*)]. Backbone residues are colored from red ($S^2 = 0.750$) to orange ($S^2 = 0.875$) to yellow ($S^2 = 1.00$) with linear interpolation. Prolines or residues whose relaxation parameters could not be quantitated due to low peak intensity or resonance overlap are colored in gray. The active site, N- and C-termini, and selected secondary structure elements are indicated to orient the reader. The figure was constructed with the program MolMol (*93*).

Conformational motions occurring on the chemical shift time scale can give rise to line broadening of the NMR resonance. A striking feature of RNase A is the large number of residues that require a chemical exchange term, R_{ex} (models 3 and 4), to achieve an adequate fit from the model-free analysis. The number of exchanging residues in RNase A accounts for approximately 30% of all residues that could be rigorously analyzed. Residues with a R_{ex} contribution to their R_2 value are shown in Figure 2B as a function of amino acid sequence. It is clear from the data in Figure 2B that conformational exchange broadening is pervasive throughout the RNase A molecule. The microscopic rate constant for conformational motion, k_{ex}, which manifests as excess NMR line broadening, can be quantitated using the relaxation-compensated CPMG (rcCPMG) experiment (*54*).

Conformational Exchange (Microseconds to Milliseconds). For nuclei undergoing conformational exchange, the observed R_2 relaxation rates are dependent on the pulse spacing (τ_{cp}) between 180° pulses of the CPMG pulse train. Interpretation of data from the classical CPMG experiment, at multiple τ_{cp} values, is complicated by the difference in relaxation rates between in-phase and anti-phase magnetization (*66*). Fortunately, the rcCPMG (*54*) experiment allows quantitation of microscopic chemical exchange rates, k_{ex}, by rendering evolution of in-phase and anti-phase ^{15}N coherence independent of pulse spacing in a CPMG experiment (*67*), thereby allowing $R_2(1/\tau_{cp})$ to be measured at multiple effective fields (*68*). Measured values of $R_2(1/\tau_{cp})$ can be fit using eq 6 for extraction of kinetic parameters under the assumption of fast conformational exchange ($k_{ex} > \Delta\omega$) (*67*, *69*). This experiment has proven useful in determining kinetic rates for backbone conformational exchange processes (*54*, *59*, *70*) and for extracting thermodynamic parameters (*59*, *71*). The rcCPMG experiment has been elegantly extended

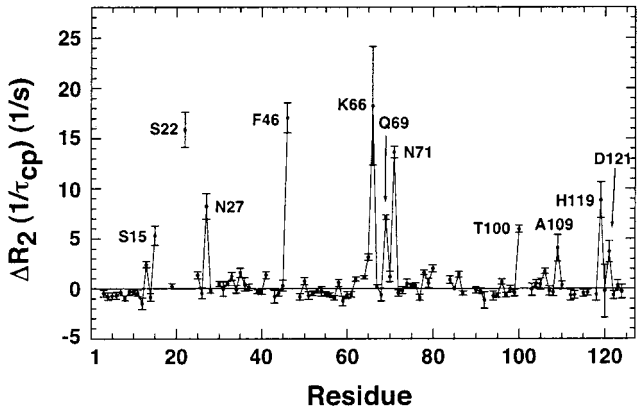

FIGURE 4: Chemical exchange in RNase A. Differences in $R_2(1/\tau_{cp})$ values are plotted as a function of amino acid sequence at 298 K. The value $\Delta R_2(1/\tau_{cp})$ was determined from the difference in measured relaxation rates for $\tau_{cp} = 10$ ms $- \tau_{cp} = 1.0$ ms. Positive values of $\Delta R_2(1/\tau_{cp})$ indicate regions of microsecond to millisecond conformational exchange. Selected residues with large values of $\Delta R_2(1/\tau_{cp})$ are labeled with the one-letter amino acid code.

to both ^{13}C- and ^{15}N-containing amino acid side chains (*60*, *72*) and more recently modified by Palmer and co-workers to increase sensitivity (*73*).

The rcCPMG experiment was applied to ^{15}N-labeled RNase A to investigate the microsecond to millisecond motions at the protein backbone level. Chemical exchange at multiple backbone sites is evident from the characteristic difference in $R_2(1/\tau_{cp})$ values measured at long (τ_{cp} =10 ms) and short ($\tau_{cp} = 1$ ms) values of the interpulse delay (Figure 4). As seen by the positive differences [$\Delta R_2(1/\tau_{cp}) > 0$] in Figure 4, conformational exchange exists throughout the RNase A structure as initially suggested by the results of the model-free analysis. A comparison of residues exhibiting chemical exchange determined from model-free analysis and from the rcCPMG experiment is shown in Figure 5 as a colored ribbon diagram. A direct quantitative comparison of R_{ex} from the two methods is not straightforward; therefore, Figure 5 is merely a qualitative indication of the spatial location of conformationally exchanging residues determined by two independent methods.

The $R_2(1/\tau_{cp})$ rates were fit to eq 6 to quantitate the microscopic conformational exchange rate. The results of these experiments for selected residues in RNase A are depicted in Figure 6. For the residues shown in Figure 6, a fit of the data to the fast limit equation (eq 6) yields k_{ex} values of 1110 $\pm$ 230 s^{-1} for His119, 1700 $\pm$ 240 s^{-1} for Gln69, and 1180 $\pm$ 320 s^{-1} for Cys65. As a control, data for Val116 are shown in which the values of $R_2(1/\tau_{cp})$ are invariant to CPMG pulse spacing, thus indicating no conformational motion for Val116 on this time scale. Data for all residues in RNase A for which the dispersion analysis could be reliably achieved are listed in Table 1. It is interesting to note that k_{ex} values for all residues are identical within experimental error.

The temperature dependence of the observed conformational motion was measured by performing the rcCPMG experiment at 283, 293, and 298 K. A plot of ln k_{ex} versus sample temperature is shown in Figure 7 for Asn71 and Cys65. The activation energy of the microsecond to millisecond motional process was determined to be 7.4 $\pm$ 3.2 kcal/mol for Asn71 and 3.6 $\pm$ 2.7 kcal/mol for Cys65 by fitting the values of k_{ex} to the linear form of the Arrhenius equation.

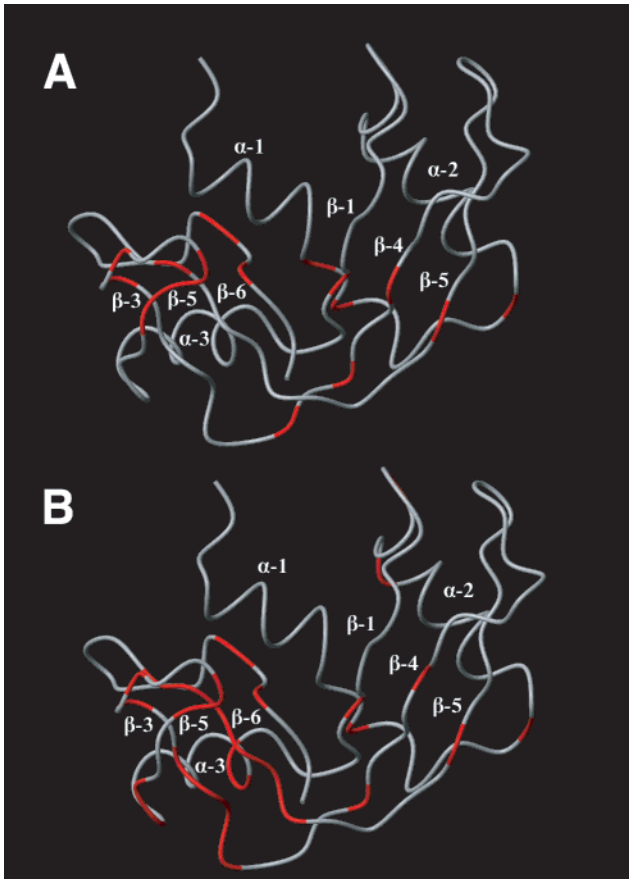

FIGURE 5: Comparison of chemical exchange in RNase A. Residues undergoing chemical exchange are colored red. In (A), residues with $\Delta R_2(1/\tau_{cp})$ greater than 1.5 s^{-1} are considered to be in exchange. In (B), residues were colored red if model 3 or 4 was an appropriate description of the spin relaxation data determined from the model-free analysis. Selected secondary structure regions are labeled to orient the reader.

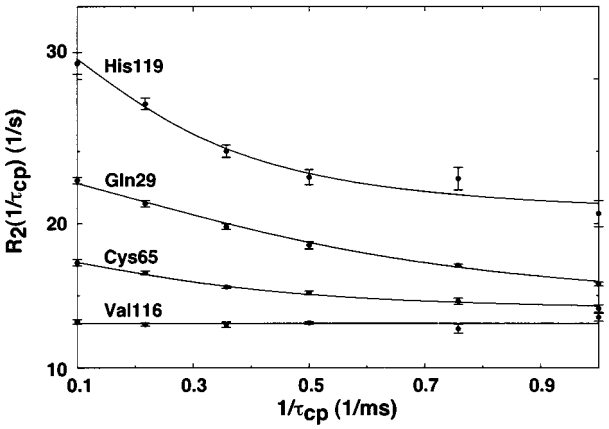

FIGURE 6: Dispersion curves for RNase A. $R_2(1/\tau_{cp})$ values as a function of $1/\tau_{cp}$ were fit to eq 6 describing a fast chemical exchange process. Data are shown for three residues that exhibit chemical exchange (His119, Gln69, and Cys65) and one residue (Val116) in which no dispersion is observed. The temperature in these experiments was kept constant at 298 K.

DISCUSSION

Conformational fluctuations are an integral aspect of enzyme-catalyzed reactions. It is imperative to uncover the

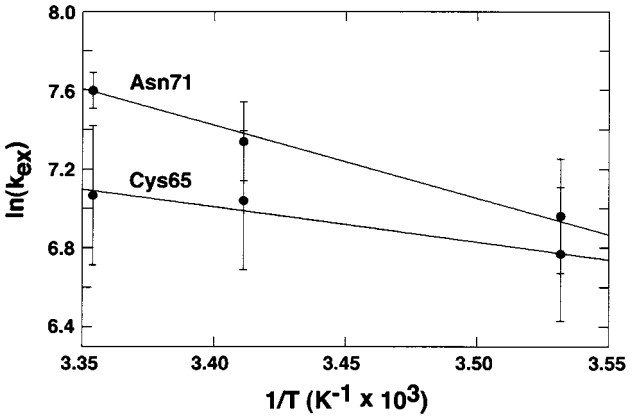

FIGURE 7: Temperature dependence of conformational exchange. The calculated chemical exchange rate, k_{ex}, is plotted versus the inverse of the absolute temperature. The data were fitted to the Arrhenius equation, in which the slope of the fitted line $= E_a/R$, where R is the gas constant; T is the temperature in kelvin. The temperature of the NMR sample was calibrated prior to each experiment using 100% methanol as the calibration standard.

details of these motions to more fully elucidate their role in enzyme function. The results of these studies identify millisecond motion in key residues in RNase A. The time scale and thermodynamics of this motion are similar to the kinetic and activation barrier for the overall catalytic reaction.

In addition to performing these experiments at pH = 6.4 where RNase A exhibits maximal activity (*65*), other aspects of these solution conditions are worth noting. No buffer was used in these experiments. RNase A is known to weakly bind small buffer molecules such as acetate, formate, and phosphate (*74*). The transient interaction between RNase A and these molecules could manifest itself, in NMR experiments, as a chemical exchange process. To avoid this potentially complicating factor, we excluded these buffer molecules from our NMR sample. Thus, the conformational motions described herein can be considered natural motions of RNase A. High ionic strength has been shown to have a negative effect on RNase A's ability to bind ligand and to catalyze its reaction (*74*, *75*). So that future NMR studies can directly compare these results to those in which RNase A is interacting maximally with ligand, the salt concentration in these experiments was kept at a minimum (10 mM NaCl). Under these conditions the backbone assignments of RNase A at pH = 6.4 were somewhat different from those reported at pH = 4.6 (*39*). As shown in the Supporting Information, the residue-specific differences in the absolute value of ^{15}N chemical shifts between pH = 4.5 and pH = 6.4 described in this work are similar to differences in chemical shifts for RNase A observed in the absence and presence of the inhibitor 2′,5′-CpA (*33*). These data suggest that RNase A exists in at least two equilibrium conformations in solution.

Fast Picosecond to Nanosecond Motions. The use of R_1, R_2, and NOE experiments to analyze configurational motion on time scales similar to the nuclear Larmor precession frequency is well documented and is typically performed using model-free analysis or spectral density mapping techniques (*9*, *10*, *61*, *62*, *76*−*82*). Here, we use NMR spin relaxation measurements and the model-free analysis to determine the amplitude of fast time scale motions in RNase A. Throughout the RNase A sequence, S^2 values are high and relatively uniform. Values of S^2 can be cautiously interpreted as a measure of the angular excursion of the N−H bond vector through the relation $S^2 = [\cos(\alpha)(1 + \cos(\alpha))/2]^2$. In this equation, α is the semiangle for a vector undergoing free diffusion in a cone (*61*, *62*). An order parameter of 0.9 therefore corresponds to a semiangle of 15°. These data indicate that, for RNase A, the conformational space accessed by the amide N−H vector on the picosecond to nanosecond time scale is quite restricted. These results are not surprising given the documented stability and robust nature of RNase A (*16*, *83*). Three residues exhibit significant deviation from this general observation, Ser22 ($S^2 = 0.809 \pm 0.021$), Glu49 ($S^2 = 0.667 \pm 0.008$), and Asn113 ($S^2 = 0.729 \pm 0.024$). Of these, only Ser22 is even modestly conserved across RNase A species. This anomalous behavior does not appear to be artifactual, and two of these residues (Ser22 and Asn113) also have higher than average crystallographic *B*-factors at the amide nitrogen position (*48*). None of these residues has been documented as being crucial for substrate binding or catalysis; the functional importance, if any, for this flexibility is unclear.

Conformational Exchange. In contrast to the apparent absence of flexibility on the fast time scale (picoseconds to nanoseconds), mobility on the slower, microsecond to millisecond time scale exists throughout the protein. The evidence for microsecond to millisecond motion is, in part, supported by the necessity of the inclusion of R_{ex} terms (models 3 and 4) for successful model-free fitting of the spin relaxation data. As stated previously, nearly one-third of the backbone residues in RNase A exhibit some conformational exchange on this slower time scale. Many of the residues exhibiting conformational motion are located in the active site and substrate binding sites.

RNase A is a somewhat oval-shaped molecule with a deep active site pocket. The bottom of the pocket is formed by three antiparallel β-sheets. The entrance to the active site cleft is flanked by the N-terminal helix (α1) and the C-terminal strand (β6). These two components of secondary structure contain the catalytically essential residues His12, His119, and Asp121. As depicted in Scheme 1, His119 is one of the two primary residues involved in phosphate cleavage. The side chain carboxylate of the invariant residue Asp121 participates in a hydrogen bond with the Nϵ2 of His119 and is important for proper positioning of this residue for catalysis (*84*). His119 and Asp121 have identical microscopic exchange rates (Table 1), which suggests that the motions of these two residues may be coordinated. These two active site residues are positioned near the B2 subsite loop, which contains residues Gln69, Glu111, and Asn71. Gln69 and Asn71 undergo a conformational exchange process with rates equal to those of His119 and Asp121 (Table 1). Conformational exchange rates are identical, within error, for the 16 residues where quantitation of k_{ex} values was reliable, suggesting a single global motional process. A physical linkage between the active site, P0, and the B2 subsite is partially provided through interaction of Asp121 with Asn67 via an intervening water molecule. Asn67 is located between the P1 and B2 subsites and thus could represent a mechanism whereby motion at one site is communicated to distant sites.

The P0 subsite also shows clear evidence of microsecond to millisecond motion. Lysine 66 resides at the P0 subsite,

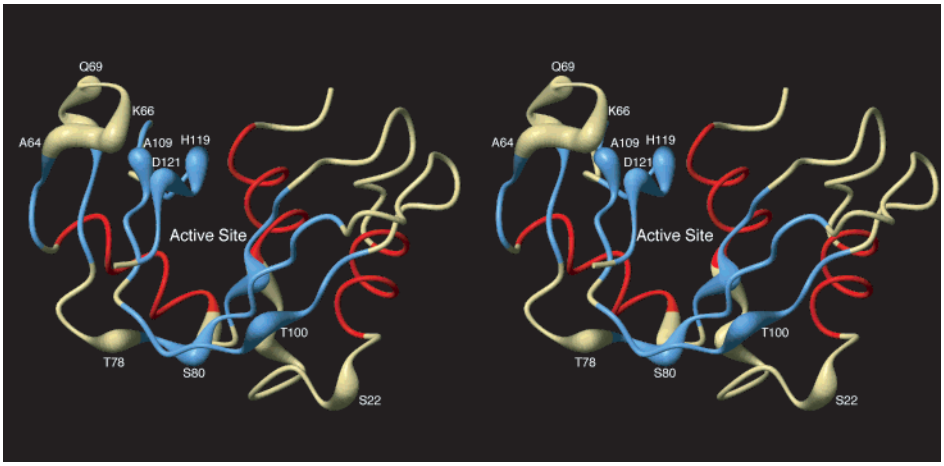

FIGURE 8: Stereo diagram depicting chemical exchange in RNase A. Residues in RNase A in which k_{ex} could be quantitated (Table 1) from the rcCPMG experiment are indicated as having a larger ribbon diameter. Secondary structure elements are color coded as follows: blue = β-sheet, red = α-helix, and gold = loops and turns. Selected exchanging residues are indicated with the one-letter amino acid code.

Scheme 2: Schematic of β-Strands in RNase A Showing Adjacency of Many of the Residues Undergoing Conformational Exchange in RNase A[a]

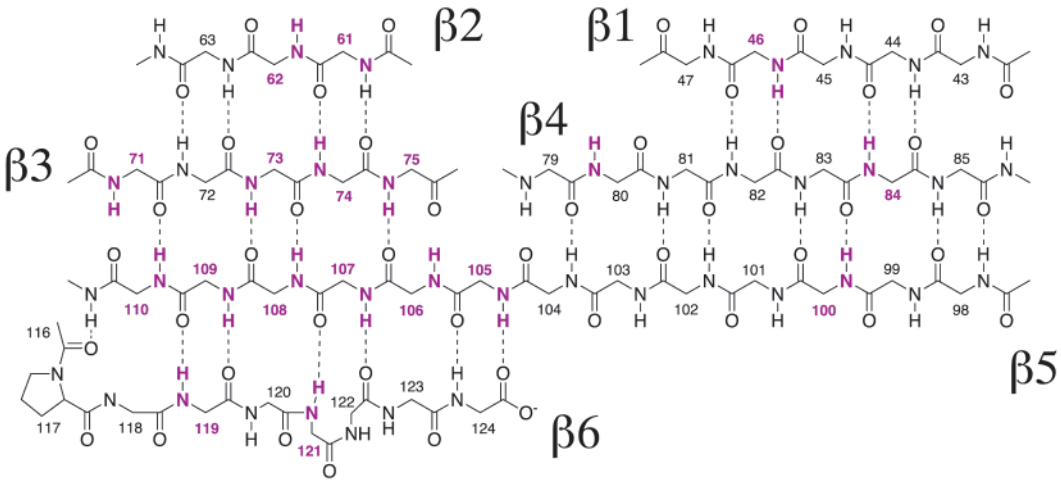

[a] Amide groups that require an R_{ex} term for successful model- free fitting are depicted in purple.

which is responsible for interactions with the substrate phosphate group located 5′ from the scissile bond. In addition to the aforementioned interaction with Asn67, the Oδ2 group of Asp121 is hydrogen bonded to the amide nitrogen of Lys66. Coupling of dynamics between P1 and P0 sites could potentially occur through this interaction.

Conformational mobility is also evident at the B1 subsite. Amino acid residues located at this site are responsible for conferring RNase A with specificity for pyrimidines. The two most crucial residues at this site are Thr45 and Asp83. Both residues display evidence of conformational motion; both show exchange broadening and increasing values of $R_2(1/\tau_{cp})$ with increasing τ_{cp} times. The signal to noise of these residues was such that accurate quantitation of microscopic exchange rates was not possible. However, the relaxation behavior of Phe46, the residue adjacent to Thr45, is well fit by eq 6. Residues near Asp83, such as Cys84, also require a chemical exchange term for successful model-free fitting. These data demonstrate that the active site and the binding sites, P0, B1, and B2, undergo motion with identical rate constants. The location of the flexible residues in RNase A are shown in Figure 8 as larger diameter ribbon renderings. In addition to the flexible active and subsite regions, the bottom of the active site contains a "band" of conformationally mobile residues located in β-sheets 1, 4, and 5. These residues could represent a hinge point upon which changes in the active site dimensions could be achieved. Scheme 2 shows a two-dimensional representation of these β-sheets in RNase A. The colored amides in this figure are those in which microsecond to millisecond flexibility has been identified from model-free analysis. Scheme 2 illustrates the connectivity between flexible residues and suggests a possible pathway for which motion at one site could be propagated to distant sites.

A comparison of enzyme kinetic rates with conformational kinetics, derived from these NMR studies, is suggestive of a correlation. The rate constant for motion measured by these NMR experiments is similar to the enzyme turnover rate (k_{cat}) of 1900 ± 130 s^{-1} (*40*). The transphosphorylation step is the fast kinetic step in the RNase A reaction while hydrolysis occurs at a rate several orders of magnitude slower (*85*). Thus the conformational motion observed in these NMR studies is rapid relative to hydrolysis and of similar magnitude to the transphosphorylation rate. It is important to note that these experiments were performed in the absence of substrate; whether these motions exist when RNase A is bound to

ligand is not known and is currently under investigation.

To assess the thermodynamics of this conformational motion in RNase A, we have measured the activation barrier through a series of temperature-dependent rcCPMG experiments. The results of this experiment are shown in Figure 7. For the two residues shown in Figure 7, the activation barrier is 3.6 ± 2.7 kcal/mol for Cys65 and 7.4 ± 3.2 kcal/mol for Asn71. These values compare to activation energies for catalysis of 7.9 kcal/mol (*86*, *87*); therefore, the barrier to the conformational motion described herein would not represent a thermodynamic limitation to catalysis. Due to resonance overlap at lower temperatures and decreased signal to noise as a result of the chemical exchange phenomena, we were unable to accurately quantitate the activation barrier for more residues. We are currently working on methods to overcome these deficiencies.

In summary, through the use of NMR spin relaxation experiments we have characterized the conformational motion in RNase A on the microsecond to millisecond time scale. The flexible residues in RNase A are located throughout the enzyme but are particularly concentrated at the active site and substrate subsites. This is suggestive evidence for the existence of motional coordination between binding and catalytic sites. To ascribe this motion to a particular step in the RNase A reaction, additional experiments performed in the presence of substrate, inhibitor, and product are warranted (*88*−*92*) and are currently in progress. Our results here indicate that RNase A has innate flexibility with kinetic and thermodynamic parameters not inconsistent with a role in enzyme function.

ACKNOWLEDGMENT

We thank Professor Mark Rance (University of Cincinnati) for providing Varian pulse sequences for measurement of R_1, R_2, and NOE values, Professor Fred Richards (Yale University) for helpful discussions, and Professor Ronald T. Raines (University of Wisconsin−Madison) for providing the expression plasmid for ribonuclease A.

SUPPORTING INFORMATION AVAILABLE

One table with residue-specific outputs from Model Free 4.01, one figure showing the RNase A sequence-dependent differences in [^{15}N]amide chemical shifts for pH = 6.4 and pH = 4.5, one table comparing identification of chemically exchanging residues as determined from model-free analysis and from the rcCPMG experiment, and the amino acid sequence of RNase A with residue-specific secondary structure (included to aid the reader in determining the location of residues in the ribbon diagrams in RNase A). This material is available free of charge via the Internet at http://pubs.acs.org.

REFERENCES

1. McCammon, J. A., and Harvey, S. C. (1987) *Dynamics of Proteins and Nucleic Acids*, Cambridge University Press, Cambridge.
2. Babu, Y. S., Bugg, C. E., and Cook, W. J. (1988) *J. Mol. Biol. 204*, 191−204.
3. Ikura, M., Clore, G. M., Gronenborn, A. M., Zhu, G., Klee, C. B., and Bax, A. (1992) *Science 256*, 632−638.
4. Lolis, E., Alber, T., Davenport, R. C., Rose, D., Hartman, F. C., and Petsko, G. A. (1990) *Biochemistry 29*, 6609−6618.
5. Lolis, E., and Petsko, G. A. (1990) *Biochemistry 29*, 6619−6625.
6. Seeholzer, S. H., and Wand, A. J. (1989) *Biochemistry 28*, 4011−4020.
7. Jackson, S. E. (1998) *Folding Des. 3*, R81.
8. Voet, D., and Voet, J. G. (1990) *Biochemistry*, John Wiley and Sons, New York.
9. Kay, L. E. (1998) *Nat. Struct. Biol. (NMR Suppl.) 5*, 513−517.
10. Palmer, A. G. (1997) *Curr. Opin. Struct. Biol. 7*, 732−737.
11. Palmer, A. G., Kroenke, C. D., and Loria, J. P. (2001) *Methods Enzymol. 339*, 204−238.
12. Richards, F. M., and Wyckoff, H. W. (1971) in *The Enzymes* (Boyer, P. D., Ed.) pp 647−806, Academic Press, New York.
13. Raines, R. T. (1998) *Chem. Rev. 98*, 1045−1066.
14. Berman, H. M., Westbrook, J., Feng, Z., Gilliland, G. L., Bhat, T. N., Weissig, H., Shindyalov, I. N., and Bourne, P. E. (2000) *Nucleic Acids Res. 28*, 235−242.
15. Mikulski, S. M., Viera, A., Deptala, A., and Darzynkiewicz, Z. (1998) *Int. J. Oncol. 13*, 633−644.
16. Kunitz, M., and McDonald, M. R. (1953) *Biochem. Prep. 3*, 9−19.
17. Jensen, D. E., and von Hippel, P. H. (1976) *J. Biol. Chem. 251*, 7198−7214.
18. Record, M. T., Jr., Ha, J. H., and Fisher, M. A. (1991) *Methods Enzymol. 208*, 291−343.
19. Aguilar, C. F., Thomas, P. J., Moss, D. S., Mills, A., and Palmer, R. A. (1991) *Biochim. Biophys. Acta 118*, 6−20.
20. McPherson, A., Brayer, G., Cascio, D., and Williams, R. (1986) *Science 232*, 765−768.
21. Katoh, H., Yoshinaga, M., Yanagita, T., Ohgi, K., Irie, M., Beintema, J. J., and Meinsma, D. (1986) *Biochim. Biophys. Acta 873*, 367−371.
22. Rushizky, G. W., Sober, H. A., and Knight, C. A. (1961) *J. Biol. Chem. 236*, 2732−2737.
23. Messmore, J. M., Fuchs, D. N., and Raines, R. T. (1995) *J. Am. Chem. Soc. 117*, 8057−8060.
24. Harris, G. W., Borkakoti, N., Moss, D. S., Palmer, R. A., and Howlin, B. (1987) *Biochim. Biophys. Acta 912*, 348−356.
25. Kim, E. E., Varadarajan, R., Wyckoff, H. W., and Richards, F. M. (1992) *Biochemistry 31*, 12304−12314.
26. Martin, P. D., Doscher, M. S., and Edwards, B. F. (1987) *J. Biol. Chem. 262*, 15930−15938.
27. Nachman, J., Miller, M., Gilliland, G. L., Carty, R., Pincus, M., and Wlodawer, A. (1990) *Biochemistry 29*, 928−937.
28. Rico, M., Santoro, J., Gonzalez, C., Bruix, M., Neira, J. L., Nieto, J. L., and Herranz, J. (1991) *J. Biomol. NMR 1*, 283−298.
29. Santoro, J., Gonzalez, C., Bruix, M., Neira, J. L., Nieto, J. L., Herranz, J., and Rico, M. (1993) *J. Mol. Biol. 229*, 722−734.
30. Wlodawer, A., and Sjolin, L. (1983) *Biochemistry 22*, 2720−2728.
31. Borkakoti, N. (1983) *Eur. J. Biochem. 132*, 89−94.
32. de Mel, V. S., Doscher, M. S., Martin, P. D., and Edwards, B. F. (1994) *FEBS Lett. 349*, 155−160.
33. Toiron, C., Gonzalez, C., Bruix, M., and Rico, M. (1996) *Protein Sci. 5*, 1633−1647.
34. French, T. C., and Hammes, G. G. (1965) *J. Am. Chem. Soc 87*, 4669−4673.
35. Alexandrescu, A. T., Rathgeb-Szabo, K., Rumpel, K., Jahnke, W., Schulthess, T., and Kammerer, R. A. (1998) *Protein Sci. 7*, 389−402.
36. Allerhand, A., Doddrell, D., Glushko, V., Cochran, D. W., Wenkert, E., Lawson, P. J., and Gurd, F. R. N. (1971) *J. Am. Chem. Soc. 93*, 544−546.
37. Brunger, A. T., Brooks, C. L. I., and Karplus, M. (1985) *Proc. Natl. Acad. Sci. U.S.A. 82*, 8458−8462.
38. Dubins, D. N., Filfil, R., Macgregor, R. B., and Chalikian, T. V. (2000) *J. Phys. Chem. B 104*, 390−401.
39. Shimotakahara, S., Rios, C. B., Laity, J. H., Zimmerman, D. E., Scheraga, H. A., and Montelione, G. T. (1997) *Biochemistry 36*, 6915−6929.
40. delCardayre, S. B., Ribo, M., Yokel, E. M., Quirk, D. J., Rutter, W. J., and Raines, R. T. (1995) *Protein Eng. 8*, 261−273.

41. Kay, L. E., Ikura, M., Tschudin, R., and Bax, A. (1990) *J. Magn. Reson. 89*, 496−514.
42. Bax, A., and Ikura, M. (1991) *J. Biomol. NMR 1*, 99−104.
43. Wittekind, M., and Mueller, L. (1993) *J. Magn. Reson. 101*, 201−205.
44. Grzesiek, S., and Bax, A. (1992) *J. Am. Chem. Soc. 114*, 6291−6293.
45. Marion, D., Driscoll, P. C., Kay, L. E., Wingfield, P. T., Bax, A., Gronenborn, A. M., and Clore, G. M. (1989) *Biochemistry 28*, 6150−6156.
46. Marion, D., Kay, L. E., Sparks, S. W., Torchia, D. A., and Bax, A. (1989) *J. Am. Chem. Soc. 111*, 1515−1517.
47. Zuiderweg, E. R., and Fesik, S. W. (1989) *Biochemistry 28*, 2387−2391.
48. Wlodawer, A., Svensson, L. A., Sjolin, L., and Gilliland, G. L. (1988) *Biochemistry 27*, 2705−2717.
49. Kay, L. E., Keifer, P., and Saarinen, T. (1992) *J. Am. Chem. Soc. 114*, 10663−10665.
50. Kordel, J., Skelton, N. J., Akke, M., Palmer, A. G., and Chazin, W. J. (1992) *Biochemistry 31*, 4856−4866.
51. Skelton, N. J., Palmer, A. G., Akke, M., Kördel, J., Rance, M., and Chazin, W. J. (1993) *J. Magn. Reson. 102*, 253−264.
52. Delaglio, F., Grzesiek, S., Vuister, G. W., Zhu, G., Pfeifer, J., and Bax, A. (1995) *J. Biomol. NMR 6*, 277−293.
53. Goddard, T. D., and Kneller, D. G., *SPARKY 3*, University of California, San Francisco.
54. Loria, J. P., Rance, M., and Palmer, A. G. (1999) *J. Am. Chem. Soc. 121*, 2331−2332.
55. Carver, J. P., and Richards, R. E. (1972) *J. Magn. Reson. 6*, 89−105.
56. Davis, D. G., Perlman, M. E., and London, R. E. (1994) *J. Magn. Reson. 104*, 266−275.
57. Ishima, R., and Torchia, D. A. (1999) *J. Biomol. NMR 15*, 369−372.
58. Luz, Z., and Meiboom, S. (1963) *J. Phys. Chem. B 39*, 366.
59. Millet, O. M., Loria, J. P., Kroenke, C. D., Pons, M., and Palmer, A. G. (2000) *J. Am. Chem. Soc. 122*, 2867−2877.
60. Mulder, F. A., Skrynnikov, N. R., Hon, B., Dahlquist, F. W., and Kay, L. E. (2001) *J. Am. Chem. Soc. 123*, 967−975.
61. Lipari, G., and Szabo, A. (1982) *J. Am. Chem. Soc. 104*, 4546−4559.
62. Lipari, G., and Szabo, A. (1982) *J. Am. Chem. Soc. 104*, 4559−4570.
63. Mandel, A. M., Akke, M., and Palmer, A. G. (1995) *J. Mol. Biol. 246*, 144−163.
64. Palmer, A. G., Rance, M., and Wright, P. E. (1991) *J. Am. Chem. Soc. 113*, 4371−4380.
65. del Rosario, E. J., and Hammes, G. G. (1969) *Biochemistry 8*, 1884−1889.
66. Orekhov, V., Pervushin, K. V., and Arseniev, A. S. (1994) *Eur. J. Biochem. 219*, 887−896.
67. Gutowsky, H. S., Vold, R. L., and Wells, E. J. (1965) *J. Chem. Phys. 43*, 4107−4125.
68. Ishima, R., Wingfield, P. T., Stahl, S. J., Kaufman, J. D., and Torchia, D. A. (1998) *J. Am. Chem. Soc. 120*, 10534−10542.
69. Allerhand, A., Gutowsky, H. S., Jonas, J., and Meinzer, R. A. (1966) *J. Am. Chem. Soc. 88*, 3185−3193.
70. Loria, J. P., Rance, M., and Palmer, A. G. (1999) *J. Biomol. NMR 15*, 151−155.
71. Mulder, F. A., Mittermaier, A., Hon, B., Dahlquist, F. W., and Kay, L. E. (2001) *Nat. Struct. Biol. 8*, 932−935.
72. Skrynnikov, N. R., Mulder, F. A., Hon, B., Dahlquist, F. W., and Kay, L. E. (2001) *J. Am. Chem. Soc. 123*, 4556−4566.
73. Wang, C., Grey, M. J., and Palmer, A. G. (2001) *J. Biomol. NMR 21*, 361−366.
74. Fedorov, A. A., Joseph-McCarthy, D., Fedorov, E., Sirakova, D., Graf, I., and Almo, S. C. (1996) *Biochemistry 35*, 15962−15979.
75. Fisher, B. M., Schultz, L. W., and Raines, R. T. (1998) *Biochemistry 37*, 17386-17401.
76. Ishima, R., and Torchia, D. A. (2000) *Nat. Struct. Biol. 7*, 740−743.
77. Li, Z., Raychaudhuri, S., and Wand, A. J. (1996) *Protein Sci. 5*, 2647−2650.
78. Farrow, N. A., Zhang, O., Szabo, A., Torchia, D. A., and Kay, L. E. (1995) *J. Biomol. NMR 6*, 153−162.
79. Ishima, R., and Nagayama, K. (1995) *J. Magn. Reson. 108*, 73−76.
80. Ishima, R., and Nagayama, K. (1995) *Biochemistry 34*, 3162−3171.
81. Peng, J. W., and Wagner, G. (1992) *J. Magn. Reson. 98*, 308−332.
82. Peng, J. W., and Wagner, G. (1992) *Biochemistry 31*, 8571−8586.
83. Anfinsen, C. B. (1973) *Science 181*, 223−230.
84. Quirk, D. J., Park, C., Thompson, J. E., and Raines, R. T. (1998) *Biochemistry 37*, 17958−17964.
85. Tarragona-Fiol, A., Eggelte, H. J., Harbron, S., Sanchez, E., Taylorson, C. J., Ward, J. M., and Rabin, B. R. (1993) *Protein Eng. 6*, 901−906.
86. Cheung, C.-C. S., and Abrash, H. I. (1964) *Biochemistry 3*, 1883−1889.
87. Eftink, M. R., and Biltonen, R. (1983) *Biochemistry 22*, 5140−5150.
88. Munagala, N., Basus, V. J., and Wang, C. C. (2001) *Biochemistry 40*, 4303−4311.
89. Osborne, M. J., Schnell, J., Benkovic, S. J., Dyson, H. J., and Wright, P. E. (2001) *Biochemistry 40*, 9846−9859.
90. Rozovsky, S., Jogl, G., Tong, L., and McDermott, A. E. (2001) *J. Mol. Biol. 310*, 271−280.
91. Rozovsky, S., and McDermott, A. E. (2001) *J. Mol. Biol. 310*, 259−270.
92. Williams, J. C., and McDermott, A. E. (1995) *Biochemistry 34*, 8309−8319.
93. Koradi, R., Billeter, M., and Wuthrich, K. (1996) *J. Mol. Graphics 14*, 29−32, 51−55.
94. Aguilar, C. F., Thomas, P. J., Mills, A., Moss, D. S., and Palmer, R. A. (1992) *J. Mol. Biol. 224*, 265−267.

BI025655M